

# Wavelength Dependence of Metal-Enhanced Fluorescence

Yongxia Zhang, Anatoliy Dragan, and Chris D. Geddes\*

*Institute of Fluorescence, Laboratory for Advanced Medical Plasmonics, and Laboratory for Advanced Fluorescence Spectroscopy, University of Maryland Biotechnology Institute, 701 East Pratt Street, Baltimore, Maryland 21202*

Received: January 19, 2009; Revised Manuscript Received: May 26, 2009

In this paper, metal-enhanced fluorescence (MEF) from 6-propionyl-2-dimethylaminonaphthalene (Prodan) in different solvents when placed in close proximity to silver island films (SIFs), surface-deposited nanoparticles, is studied. We observe that MEF is wavelength dependent: the enhanced emission of Prodan on SIFs in different solvents changes from 1.5- to 3-fold as compared to a glass control sample containing no silver nanoparticles. Our findings strongly suggest that MEF of Prodan in different solvents is correlated with the scattering portion of the extinction spectrum for metallic particles, i.e., the fluorophore couples and radiates through that scattering mode, which further confirms our laboratories current interpretation of the MEF effect.

## Introduction

Fluorophore photophysical properties, including intensity, lifetime, and photostability, have been modified by incorporating sub-wavelength-sized metallic nanostructures in close proximity to excited states.<sup>1</sup> There are currently several mechanisms for the near-field interactions of fluorophores with metallic nanoparticles. Fluorophore photophysical properties were originally thought to be modified by a resonance interaction by their close proximity to surface plasmons, which gives rise to a modification of the fluorophore radiative decay rate.<sup>2</sup> This description was fueled by earlier workers who had shown increases in fluorescence emission coupled with a simultaneous drop in radiative lifetime,<sup>3</sup> which can be explained by a fluorophore radiative decay rate modification when using a classical fluorescence description.<sup>4</sup> However, our laboratories current interpretation of metal-enhanced fluorescence (MEF) is described by a model whereby nonradiative energy transfer occurs from excited distal fluorophores, to the surface plasmon electrons in noncontinuous films, in essence a fluorophore through-space induced mirror dipole in the metal. The surface plasmons in turn, then radiate the emission (quanta) of the coupling fluorophore<sup>5–7</sup> (Figure 1, top). This explanation has been facilitated by the observation of surface plasmon coupled fluorescence (SPCF), whereby fluorophores distal to a continuous metallic film can directionally radiate fluorophore emission at a unique angle from the back metallic film,<sup>8</sup> also a result of dipole induced surface plasmons in the near-field, i.e., <200 nm.<sup>5,9</sup> In the first unified plasmon fluorophore description postulated by Geddes,<sup>10</sup> MEF is partially attributed to the scattering portion of the extinction spectrum for metallic particles, i.e., a fluorophore couples to that scattering mode (Figure 1, bottom). Larger particles (>100 nm) have a more substantial scattering component to their extinction spectrum, which accounts for even greater MEF. At present, MEF is thought to be comprised of two cooperative mechanisms and near-field interactions: (1) an electric field effect and (2) an induced plasmon effect. In the so-called electric field effect, fluorophores in close proximity (<10 nm) to plasmonic nanoparticles are exposed to the increased electric fields in between

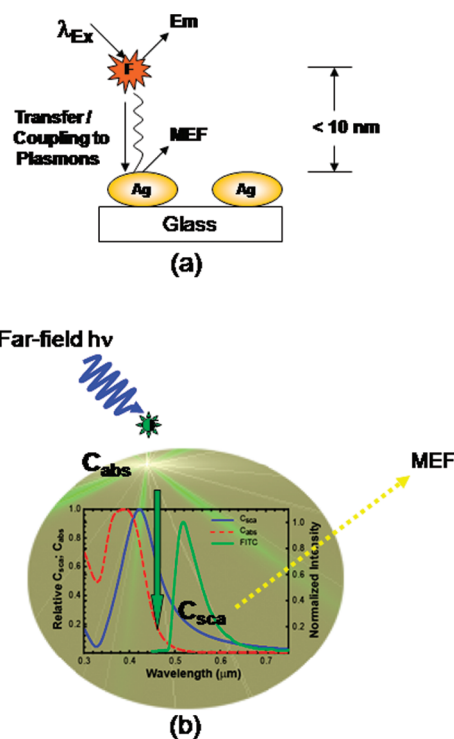


**Figure 1.** Graphical representation of current interpretation for MEF on silver nanostructures (a). Relative absorption and scattering cross sections for 100 nm colloid with overlaid normalized FITC emission spectra (b). The figure depicts coupled emission radiating through the nanoparticles scattering mode.

and around the nanoparticles, effectively resulting in significant increases in their absorption cross section.<sup>4</sup> This lends itself to a subsequent increase in the excitation and eventually in the fluorescence emission of the fluorophores, noting that the fluorescence lifetime remains unchanged. In the second mechanism, where the excited state energies of fluorophores are partially transferred to surface plasmons (induced surface plasmons), two distinct observations can be made for fluorescent species in close proximity to plasmonic nanoparticles: (1) an increase in the fluorescence emission from the metal–fluorophore *unified system* with the spectral properties of the fluorophores

\* To whom correspondence should be addressed. E-mail: geddes@umbi.umd.edu.

maintained and (2) a reduction in the excited -state decay time (fluorescence lifetime), which invariably gives rise to improvements in the photostability of the fluorophores, due to their spending less time in a reactive excited state.

In the past 5 years, we have studied many factors that can influence the magnitude of the MEF phenomenon, such as the use of different metals including silver,<sup>11</sup> gold,<sup>12,13</sup> copper,<sup>14</sup> chromium,<sup>6</sup> and zinc,<sup>15</sup> different nanostructure architectures such as silver islands films (SIFs), silver colloids, silver nanotriangles, silver nanorods, and fractal-like silvered surfaces,<sup>16</sup> the size of these nanoparticles, as well as the nature of the surrounding media, temperature, dielectric, etc.<sup>17</sup> However, our previous observations of MEF focused on fluorophores, whose spectral properties were unperturbed by the local environment. We have investigated these effects both theoretically, using numerical simulations based on the FDTD (finite difference time domain) method,<sup>18</sup> as well as experimentally.<sup>19</sup> In this paper, we subsequently report our observations of MEF from 6-propionyl-2-dimethylaminonaphthalene (Prodan) in different solvents when placed in close proximity to SIFs. Prodan displays a high sensitivity to the polarity of the local environment and its maximum emission wavelength shifts with the polarity of the solvent.<sup>20</sup> Due to Prodan's solvent sensitivity, it has been widely used to probe the polarity and hydrogen-bonding capacity of microenvironments.<sup>21</sup> For our studies of metal-enhanced fluorescence, Prodan offers the unique opportunity to study the wavelength dependence of MEF, by simply changing solvent and subsequently the Prodan emission spectrum, through which we can observe the wavelength dependence of MEF. Interestingly, our laboratory has explored the same dependence using different fluorophores,<sup>17</sup> but in these studies it was difficult to account for the changes in fluorophore quantum yield and lifetime, in addition to the changing emission maxima. For Prodan, the free space quantum yield and lifetime show only very slight changes as a function of solvent, enabling the wavelength dependence of MEF to be explored for the first time. In addition, we have undertaken numerous numerical simulations to study the effect of solvent polarity and particle size on the electric field component in MEF. Interestingly, the e-field component contributes little to the enhanced fluorescence observed, where the enhanced fluorescence signatures track well the scattering-portion of the nanoparticles' extinction spectrum, supporting our mechanism and indeed unified description for MEF<sup>7,10</sup> (Figure 1b).

## Experimental Section

**Chemicals.** Silver nitrate (99.9%), sodium hydroxide (99.996%), ammonium hydroxide (30%), D-glucose, ethanol (HPLC/spectrophotometric grade), Prodan, cyclohexane, toluene, chloroform, DMF, acetonitrile, DMSO, and fluorescein were obtained from Sigma-Aldrich. Quartz (75 × 25 mm<sup>2</sup>) slides were bought from Ted Pella, Inc. All chemicals were used as received.

**Preparation of Sandwich-Format Samples for MEF Measurements.** A solution of 300 μL of Prodan dissolved in cyclohexane, toluene, chloroform, DMF, acetonitrile, DMSO, acetonitrile/H<sub>2</sub>O = 1:1 was sandwiched between both the quartz slides and the SIFs coated quartz slides, respectively. The surfaces were illuminated with the appropriate excitation source and fluorescence emission spectra and real-color photographs of fluorescence emission were collected. SIFs (size ≈ 100 nm) were prepared according to our previously published procedure.<sup>11</sup> The morphology of the SIFs is shown in the AFM image (Figure 2a).

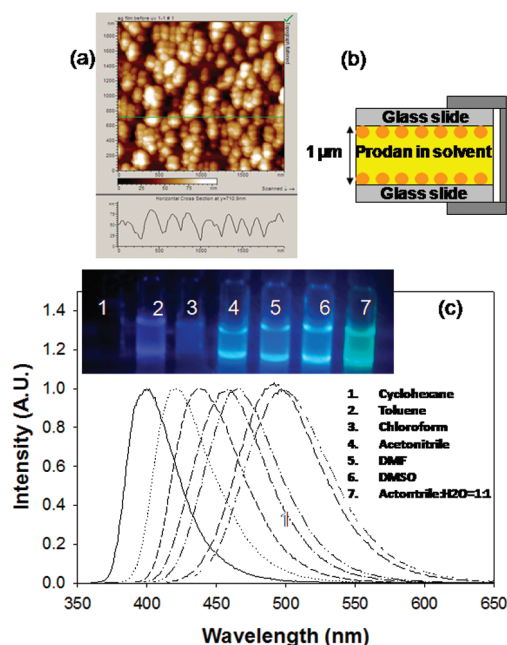


**Figure 2.** AFM image of SIFs film (a), sample sandwich geometry. (b) Normalized fluorescence emission spectra of Prodan excited at 350 nm in (1) cyclohexane, (2) toluene, (3) chloroform, (4) acetonitrile, (5) DMF (6) DMSO, and (7) acetonitrile/H<sub>2</sub>O = 1:1. (c) Ex. 350 nm. Inset: photographs of Prodan solutions when excited with a UV source.

**Optical Spectroscopy and Real-Color Photographs.** Fluorescence spectra of fluorophores on blank quartz substrates and SIFs nanostructured films were collected using an Ocean Optics HD2000 fluorometer. Excitation light was incident to the bottom of the slides surface with an excitation bandpass of 350–360 nm. Real-color photographs of fluorescence emission were taken through an emission filter with a Canon Powershot S50 digital camera.

**Frequency-Domain Phase and Modulation Measurements.** The lifetime of fluorophores was measured using a Multi-Frequency MF<sup>2</sup> Fluorometer from HORIBA Jobin Yvon. The excitation of fluorophores (in a sandwich format and front-face geometry) was performed using a 365 nm NanoLED pulsed diode with a 400 nm long-pass filter being used for the emission. Rhodamine 101 in water was used as a lifetime standard (lifetime = 4.32 ns). The frequency-domain phase and modulation values were analyzed with a monoexponential decay time model using fitting software provided by HORIBA Jobin Yvon.

**Atomic Force Microscopy (AFM).** AFM images were performed on a Molecular Imaging Picoplus microscope. Samples were imaged at a scan rate of 1 Hz with 512 × 512 pixel resolution in tapping mode.

**Mie Scattering and FDTD Calculations.** Mie scattering calculations for a 100-nm silver nanoparticle in water were performed using freeware MieCalc v1.5 software.

**FDTD Simulations.** The numerical FDTD simulations were performed for several purposes: to determine the dependence of the maximum of the electric field intensity ( $|E|^2_{\max}$ ), generated at the surface of a 100-nm silver nanoparticle upon solvent polarity; to calculate the dependence of the  $|E|^2_{\max}$  on the silver nanoparticle size in different solvents and to calculate the near-field intensity distribution as a function of distance from the nanoparticle surface. All simulations were undertaken using Lumerical FDTD Solution software (Vancouver, Canada).

For FDTD simulations, the incident field was defined as a plane wave with a wave-vector that is normal to the injection

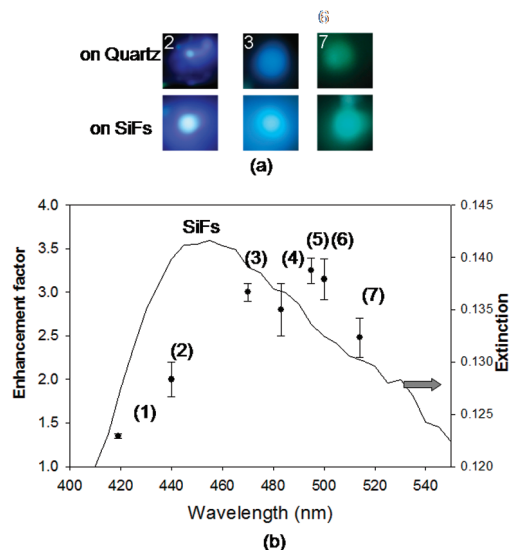


**Figure 3.** (a) Photograph of prodan on SiFs and quartz. (b) Fluorescence enhancement (factor versus different maximum emission wavelengths for Prodan in various solvents on SiFs. (1) Cyclohexane, (2) toluene, (3) chloroform, (4) DMF, (5) acetonitrile, (6) DMSO, (7) acetonitrile/H<sub>2</sub>O = 1:1.

surface, and scattered and total fields were monitored during the simulation. The simulation region was set to  $650 \times 650$  nm<sup>2</sup> with high mesh accuracy. To minimize simulation times and maximize the resolution of the field enhancement regions around the silver particle, a mesh override region was set to 0.1 nm around the Ag particle (nanoparticle size was varied; maximum size was 500 nm). The overall simulation time was set to 200 fs and calculated over a frequency range of 300–400 nm, where a plasma model was used to represent the properties of the silver nanoparticle in the range of 300–400 nm. For other FDTD simulations the polarity of the media around the silver particle was varied, from  $n = 1.333$  (polar water) to  $n = 1.496$  (nonpolar toluene), by changing the background index in the simulation area.

## Results and Discussion

Prodan was originally characterized by Gregorio Weber, and the phenomenon of prodan's dipole relaxation was subsequently well studied.<sup>20</sup> Prodan possesses a dipole moment due to a partial charge separation between the 2-dimethylamino and the 6-carbonyl residues. The dipole moment of Prodan is increased upon excitation and can cause reorientation of a polar solvent as compared to an apolar solvent. The energy required for solvent reorientation decreases the probe's excited state energy, which is reflected in a continuous red-shift of the probe's steady-state emission spectrum. The emission spectra of Prodan in different solvents, from apolar cyclohexane with a polarity index of 0.2, to a polar solvent mixture acetonitrile/water, with a polarity index of 8, as well as the respective photographs of excited prodan in different solvents, are shown in Figure 2. A blue emission is typically observed in apolar solvents while a much more green emission characteristic in more polar solvents, Figure 2.

Photographs of prodan solvents sandwiched on SiFs and on the quartz control slides from several different solvents are shown in Figure 3, insert. It can be observed that the emission intensity is much more clearly detectable from between SiFs than from the quartz control slides, i.e., slides with no silver nanostructures. These findings of MEF of Prodan are consistent

with our previous reported findings of the emission from other fluorophores sandwiched between silver nanostructures.<sup>22</sup> Subsequently, the MEF factors for Prodan in different solvents versus emission wavelength are summarized in Figure 3b. We observed that the maximum emission wavelength of Prodan on SiFs is slightly red-shifted as compared to solution, i.e., Prodan in cyclohexane solution  $\approx 400$  nm, on SiFs  $\approx 419$  nm. Interestingly, this is the first report of a spectral shift for a fluorophore located near to silver and is to be the theme of a future paper dedicated to MEF solvent relaxation properties. We have also observed that the Plasmon absorption spectrum of the SiFs in the different solvents used only very slightly changes.

From Figure 3 we can see that the enhancement factors (numerical value of the emission from SiFs/glass) are wavelength dependent with the enhancement increasing as the solvent polarity increases. For the polar solvent acetonitrile, the enhancement emission ratio of prodan on SiFs, as compared to the control slide reached  $\sim 3$ -fold. However, for an apolar solvent such as cyclohexane, the enhancement emission ratio is  $\sim 1.5$ .

In order to understand these findings and the wavelength dependence of MEF, we first overlaid the extinction spectrum of SiFs with the enhancement factor trend determined for Prodan in different solvents in Figure 3b, where the experimentally determined extinction spectrum shows a maximum of  $\sim 450$  nm. As we can see, the emission enhancement factor trend for prodan *does not directly correlate* with the extinction spectrum of the SiFs. It is known that the extinction properties ( $C_E$ ) of metal particles can be expressed as both a combination of both absorption ( $C_A$ ) and scattering ( $C_S$ ) factors, when the particles are spherical and have sizes comparable to the incident wavelength of light, i.e., in the Mie limit.

$$C_E = C_A + C_S = k_1 I m(\alpha) + \frac{k_1^4}{6\pi} |\alpha|^2 \quad (1)$$

where  $k_1 = 2\pi n_1/\lambda_0$  is the wavevector of the incident light in medium  $I$  and  $\alpha$  is the polarizability of a sphere with radius  $r$ ,  $n_1$  is the refractive index, and  $\lambda_0$  the incident wavelength. The term  $|\alpha|^2$  is square of the modulus of  $\alpha$ .

$$\alpha = 4\pi r^3 (\epsilon_m - \epsilon_1) / (\epsilon_m - 2\epsilon_1) \quad (2)$$

where  $\epsilon_1$  and  $\epsilon_m$  are the dielectric and the complex dielectric constants of the metal, respectively. The first term in eq 1 represents the cross section due to absorption,  $C_A$ , and the second term, the cross section due to scattering,  $C_S$ . Our current interpretation of MEF is one underpinned by the scattering component of the metal extinction, i.e., the ability of fluorophore-coupled plasmons to radiate (plasmon scatter) as pictorially shown in Figure 1b. Intuitively, larger particles have wavelength distinctive scattering spectra ( $C_S$ ) as compared to their absorption spectra ( $C_A$ ), facilitating plasmon coupled emission from the larger nanoparticles. Quenching typically occurs when have a dominant absorption component of the extinction spectrum, which is comprised of both absorption and scattering. In this regard, we have questioned how the observed enhancement factor trend therefore correlates with the scattering portion of the extinction spectrum for the metallic particles. Subsequently, we overlaid the fluorescence enhancement factor for different maximum emission wavelengths for Prodan with the absorption and scattering spectra for a Ag colloid (100 nm)

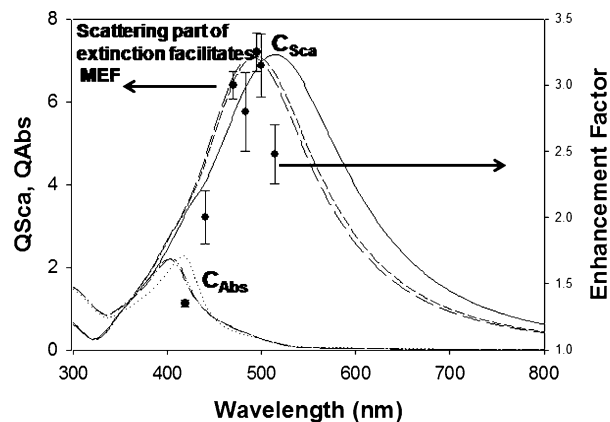


**Figure 4.** Fluorescence enhancement factor versus wavelength for Prodan in various solvents deposited on 100 nm Ag colloids. The absorption and scattering spectra are also shown for a 100 nm Ag colloid in water (refractive index, 1.333), water/acetonitrile = 1:1 (refractive index, 1.3457), toluene (refractive index, 1.49). Calculated from Mie theory.

in a water media (shown in Figure 4). Note: 100 nm size particles were typically identified in the AFM analysis of the SIFs. From Figure 4, we observe that the enhancement factor trend *correlates well* with the silver nanoparticle scattering component of the extinction.

Earlier we suggested two complementary effects for the MEF enhancement: (i) enhanced absorption (i.e., enhanced absorption cross-section) facilitates enhanced emission and (ii) surface plasmons can radiate coupled fluorescence efficiently. To further understand the enhanced absorption, we have studied the solvent-dependence of the electromagnetic field around the metal nanoparticles. When a luminophore is placed near to metal, there is often a very strong net absorption effect caused by the localized enhanced electromagnetic field of the incident excitation field. In essence, conducting metallic particles can modify the free space absorption condition in ways that increase the photonic mode density and incident electric field felt by a luminophore. Since enhanced electromagnetic fields in proximity to metal nanoparticles are the basis for the increased system absorption in MEF, we can use FDTD numerical methods to simulate the e-field distributions around silver nanoparticles in different solvents (Figure 5). As we can see, the electric field around the silver nanoparticles increases as the solvent polarity increases (Figure 5), which also supports the enhancement factor trend shown in Figure 4. The wavelength dependence of the e-field, recalling that this contributes to the enhanced absorption component in MEF, shows a decreasing and opposite trend with increased wavelength, Figure 6, with a maximum value around 450 nm. This suggests that the e-field contributes little to the enhancement factor trend observed in Figure 4.

We have also simulated the effect of nanoparticle diameter on the maximum e-field intensity induced by 360 nm incident far-field excitation, i.e., that used for Prodan excitation, where the arrows depict nanoparticle sizes which correspond to 1/4, 1/2 the wavelength of the incident field, Figure 7. FDTD calculations of the near-field intensity were also made from the surface of a 100 nm diameter silver nanoparticle. Zero distance corresponds to the first point on the particle surface. Figure 8 shows how the electric field decays as we move further away from the silver nanoparticle. Hence, Prodan within 20 nm of the SIFs is likely to show enhanced absorption properties. It should be noted that an enhanced e-field only influences the excitation rate of a fluorophore by an effective change in its

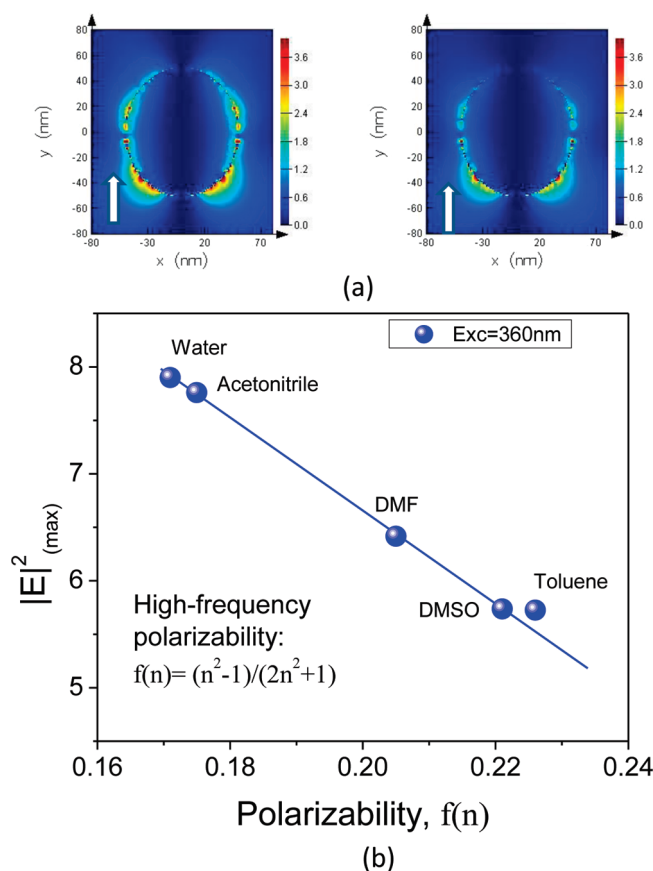


**Figure 5.** (a) Graphical images of 2D E-field distribution for silver nanoparticle surrounded by polar (water,  $n = 1.333$ ) and nonpolar (toluene,  $n = 1.496$ ) solvents. (b) The dependence of a maximum e-field intensity (incident + scattering components) upon polarizability of the media ( $f(n)$ ). The e-field calculations were undertaken using FDTD simulations for 100 nm diameter silver nanoparticle using 360 nm wavelength incident field.

absorption cross-section in the metal–fluorophore coupled system but does not influence its emissive lifetime.

For MEF, while the emission intensity of fluorophores placed in close proximity to plasmonic nanostructures is increased, the lifetime of their excited states (i.e., decay time) is expected to be reduced due to the *coupling to* and *emission from* the surface plasmons. It is thought that the very short lifetime of fluorophores near to metal is in fact the plasmon lifetime,<sup>7</sup> where the plasmons in essence radiate the coupled quanta, Figure 1, top. In this regard, the lifetime of Prodan near to SIF substrates was measured. The overall results for the lifetime of Prodan are given in Table 1. A close examination of Table 1 reveals that the lifetime of Prodan is shorter than 200 ps in cyclohexane, 1.21 ns in toluene, 1.39 ns in chloroform, 1.90 ns in acetonitrile, 2.45 ns in DMF, 2.74 ns in DMSO, and 1.23 ns in a water/acetonitrile mixture, respectively, although Prodan is sparsely soluble in the water/acetonitrile mixture. The Prodan lifetime is however much shorter for all solvents, less than 200 ps, when in close proximity to silver nanostructures (Table 1). The decrease in the fluorescence lifetime for the prodan when in the presence of metal nanostructures (Table 1), strongly suggests that the induced-plasmon effect also contributes subsequently to the fluorescence enhancement,<sup>19</sup> where >5–30 fold lifetime reductions are typically observed. The lifetime results, coupled with the observations of enhanced emission, is consistent with other reports for lumophores close to silver nanostructures reported by our laboratory.<sup>4–7</sup> It is interesting to note that the

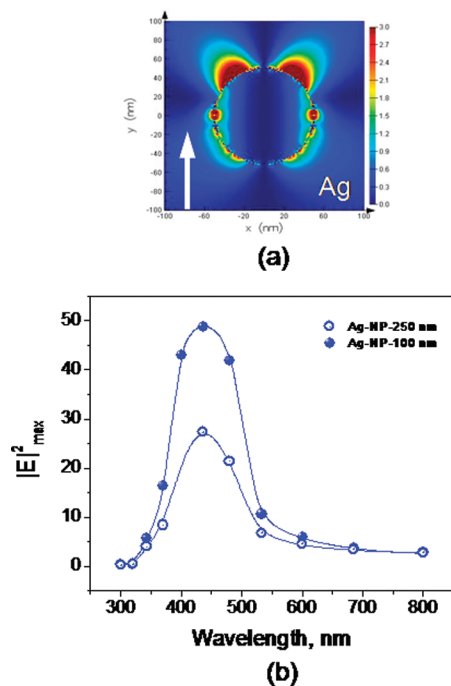


**Figure 6.** (a) Image of near-field intensity distribution around a 100 nm Ag nanoparticle. White arrow shows direction of the incident light injection. (b) The dependence of electric field maximum intensity upon wavelength of incident light for both 100 and 250 nm diameter nanoparticles. Calculations were undertaken using numerical FDTD simulations.

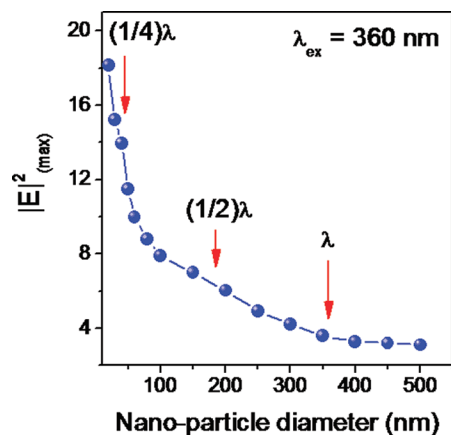


**Figure 7.** Influence of the silver nanoparticle diameter on a maximum e-field intensity induced by 360 nm incident far-field excitation. Arrows show nanoparticle sizes corresponding to 1/4, 1/2 wavelength of the incident field.

free space lifetimes in Table 1 show that the lifetime increases as the polarity index of the medium also increases. Previous reports of metal-fluorophore interactions, which have considered a radiative-rate modification as the mechanisms for the enhanced emission intensity on silver,<sup>23</sup> report that the greatest enhancements are observed for the fluorophores with the lowest free space quantum yield.<sup>23</sup> In these reports, different fluorophores are used which all have different emission spectra which will invariably have different degrees of overlap with the scattering portion of the nanoparticle extinction. Conversely, for Prodan here, the largest enhancement factors observed for silver actually occur in solvents where the free space quantum yield and lifetime are also the largest. While it is difficult to interpret past reports where solvent parameters may also account for the enhanced emission observations, it is clear here that with a

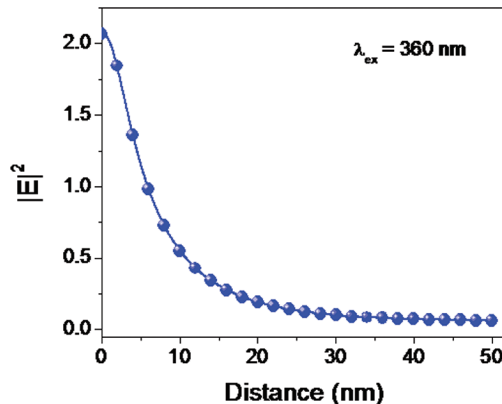


**Figure 8.** E-field intensity decay along the  $x$  axis, perpendicular to the direction of the applied incident far-field, is exponential. FDTD calculations of the near-field intensity were made from the surface of a 100 nm diameter silver nanoparticle. Zero value of the distance corresponds to the first point on the particle surface.

**TABLE 1: Fluorescence Lifetime of Prodan in Different Solvents and on SiFs Measured Using Frequency-Domain Fluorometry**

solvent	lifetime (free-space)	$\chi^2$	on SiFs (near-field)	polarity index
cyclohexane	<200 ps		<200 ps	0
toluene	1.21 ns	1.01	<200 ps	0.2
chloroform	1.39 ns	1.04	<200 ps	4.1
acetonitrile	1.90 ns	1.01	<200 ps	5.8
DMF	2.45 ns	0.9	0.66 ns	6.4
DMSO	2.74 ns	1.08	<200 ps	7.2
water/acetonitrile = 1:1	1.23 ns	1.0	0.38 ns	8

minimal e-field (e-field is greater at shorter wavelengths, i.e., Figure 6), the trends correlate with the extinction scattering spectrum as shown in Figure 4.

We have also studied the enhancement factor of FITC (Fluorescein isothiocyanate) on SiFs as a function of solvents, where fluorescein does not have solvent-dependent spectra, i.e., absorption or emission, Figure 9. As we can see, solution polarity has little to no influence on the enhancement factor. Interestingly, this also suggests that the wavelength-dependence of the electric field, and indeed its solvent dependence on the plasmon absorption and (Figure 6) have little effect on the observed enhancement factor for FITC visualized from the SiFs.

## Conclusions

In this paper, we observe that MEF is wavelength dependent: where the enhancement factors of Prodan on SiFs in different

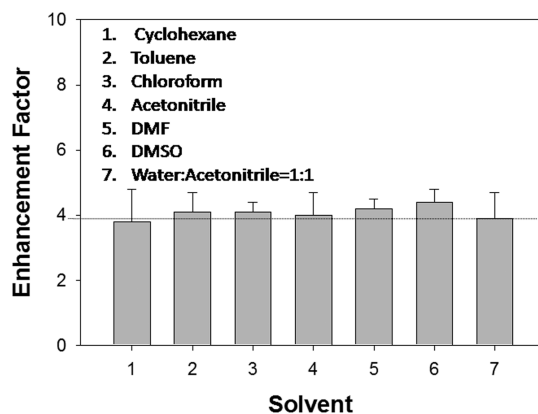


**Figure 9.** Fluorescence enhancement factor for Fluorescein in different solvents.

solvents changed from ~1.5- to 3-fold, as a function of wavelength. Our findings strongly suggest that MEF of Prodan in different solvents is correlated with the scattering portion of the extinction spectrum for metallic nanoparticles, i.e., an excited-state coupling to that scattering mode, as depicted in Figure 1, bottom. Our results also show that the wavelength dependence of the electric field, does not correlate with the observed enhancements, nor do reports that the lowest free space quantum yield of a fluorophore (i.e., in the absence of metal) gives rise to the largest enhancement factors.<sup>4</sup> Interestingly, Prodan was shown to have the largest enhancement factors for the largest lifetimes observed in solvents. Further, reports by others<sup>23,24</sup> studied systems using many dyes were both the quantum yield and emission wavelength changed, resulting in an unclear correlation between enhancement factor and wavelength. To the best of our knowledge, this is the first report of the wavelength dependence of MEF where the electrical field component is accounted for and is indeed minimal.

**Acknowledgment.** The authors thank the IoF, MBC, UMBI for salary support.

### References and Notes

- (1) Barnes, W. L. *J. Mod. Optics* **1998**, *45*, 661.
- (2) Gersten, J. I.; Nitzan, A. *Chem. Phys. Lett.* **1984**, *104*, 31.
- (3) Weitz, D. A.; Garoff, S.; Hanson, C. D.; Gramila, T. J.; Gersten, J. I. *J. Lumin.* **1981**, *24–5*, 83.
- (4) Geddes, C. D.; Lakowicz, J. R. *J. Fluoresc.* **2002**, *12*, 121.
- (5) Aslan, K.; Previte, M. J.; Zhang, Y.; Geddes, C. D. *Anal. Chem.* **2008**, *80*, 730.

- (6) Pribik, R.; Aslan, K.; Zhang, Y.; Geddes, C. D. *J. Phys. Chem. C* **2008**, *112*, 17969.
- (7) Aslan, K.; Zhang, Y. X.; Geddes, C. D. *J. Appl. Phys.* **2008**, *103*, 084307.
- (8) Liebermann, T.; Knoll, W. *Colloids Surf., A* **2000**, *171*, 115.
- (9) Previte, M. J. R.; Zhang, Y. X.; Aslan, K.; Geddes, C. D. *Appl. Phys. Lett.* **2007**, *91*.
- (10) Aslan, K.; Malyn, S. N.; Zhang, Y. X.; Geddes, C. D. *J. Appl. Phys.* **2008**, *103*, 084307.
- (11) Aslan, K.; Leonenko, Z.; Lakowicz, J. R.; Geddes, C. D. *J. Fluoresc.* **2005**, *15*, 643.
- (12) Aslan, K.; Malyn, S. N.; Geddes, C. D. *J. Fluoresc.* **2007**, *17*, 7.
- (13) Aslan, K.; Lakowicz, J. R.; Geddes, C. D. *Anal. Chem.* **2005**, *77*, 2007.
- (14) Zhang, Y.; Aslan, K.; Previte, M. J. R.; Geddes, C. D. *Appl. Phys. Lett.* **2007**, *90*, 173116.
- (15) Kadir Aslan, M. J. R. P.; Yongxia, Z.; Geddes, C. D. *J. Phys. Chem. C* **2008**, *112*, 18368.
- (16) Aslan, K.; Lakowicz, J. R.; Geddes, C. D. *Anal. Bioanal. Chem.* **2005**, *382*, 926.
- (17) Zhang, Y.; Aslan, K.; Previte, M. J.; Geddes, C. D. *J. Fluoresc.* **2007**, *17*, 627.
- (18) Chowdhury, M. H.; Gray, S. K.; Pond, J.; Geddes, C. D.; Aslan, K.; Lakowicz, J. R. *J. Opt. Soc. Am. B* **2007**, *24*, 2259.
- (19) Aslan, K.; Malyn, S. N.; Geddes, C. D. *Analyst* **2007**, *132*, 1112.
- (20) Artukhov, V. Y.; Zharkova, O. M.; Morozova, J. P. *Spectrochim. Acta, Part A* **2007**, *68*, 36.
- (21) Parasassi, T.; Kranowska, E. K.; Bagatolli, L.; Gratton, E. *J. Fluoresc.* **1998**, *8*, 365.
- (22) Zhang, Y.; Aslan, K.; Previte, M. J.; Geddes, C. D. *Appl. Phys. Lett.* **2007**, *90*, 053107.
- (23) Lakowicz, J. R. *Anal. Biochem.* **2001**, *298*, 1.
- (24) Lakowicz, J. R.; Shen, Y. B.; D'Auria, S.; Malicka, J.; Fang, J. Y.; Gryczynski, Z.; Gryczynski, I. *Anal. Biochem.* **2002**, *301*, 261.

JP9005668